

Effects of large-scale human activities on the North Sea seabed

H.H. van der Veen & S.J.M.H. Hulscher

Water Engineering & Management, University of Twente, The Netherlands

ABSTRACT: There are many plans to utilize the North Sea environment, such as large-scale sand mining for large infrastructural projects and the placement of offshore wind farms. We investigated the effects of these activities on the North Sea seabed. To do this, we set up a GIS (Geographical Information System) containing data on the North Sea and embedded an idealized morphodynamic model to calculate the large-scale morphodynamics due to sand mining and offshore wind farms in the GIS. The results show that sand mining and wind farms have a large impact on the morphodynamics of the seabed. Furthermore, the inclusion of the morphodynamic models in the GIS allows a rapid calculation of the morphological effects of these activities at a certain location in the North Sea, thus providing a rapid assessment tool regarding the large-scale morphological effects of sand mining and offshore wind farms.

1 INTRODUCTION

On the Netherlands continental shelf an average of 30 Mm³ of sand and gravel is extracted per year. In the future, the demand is likely to rise due to large projects, like the land reclamation project Maasvlakte II, and may go up to 200-2000 Mm³ over a period of 5 to 10 years depending on the plans (Hoogewoning and Boers, 2001).

Roos et al. (2007) studied the morphological effects of large-scale sand pits for varying physical characteristics and pit design parameters. To allow for comparison between the different design parameters they introduce three pit indicators, namely: degree of flow contraction, pit migration and area of morphodynamic influence. They found that a disturbance of the seabed with a certain preferred length scale can also trigger natural dynamic morphological features.

The second human activity that we investigate is offshore wind energy. The need for renewable energy is rising. The members of the European Union have committed themselves to a 21% share of renewable energy by the year 2010. Moreover, in 2004 the European Parliament has adopted a resolution that stresses the need of setting a mandatory target of a share of 20% renewable energy by the year 2020 (European Parliament, 2004). At the moment wind energy is one of the few forms of renewable energy that can be harvested efficiently. The total wind resources in the offshore area of Europe have been es-

timated at up to 3000 TWh, this is in theory sufficient to supply Europe's total current electricity demand (Danish_Energy_Authority, 2005). Additionally, as placing space onshore is scarce, many European countries are planning and realizing offshore wind farms.

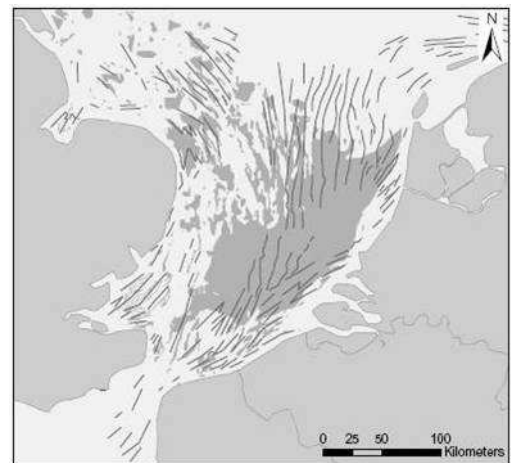


Figure 1: Overview of the southern part of the North Sea. The gray areas denote sand wave occurrence and the black lines show the locations of sand banks. Courtesy of F. van der Meer and B. Pérez Lapeña.

Several sand bank systems are present in the North Sea area, and large parts of the seabed are covered with sand waves (see

Figure 1). Sand banks have a wavelength between 1 and 10 km and can have a height of several tens of meters (Dyer and Huntley, 1999). Sand banks can ei-

ther be formed by the tide or can be remains of relict features which can be reworked by the tidal currents. Banks that are formed by the tide can be either actively maintained or moribund. Actively maintained sand banks are formed by the modern (late Holocene) tidal regime. Moribund banks are formed during periods of lower sea levels, they occur in deeper water where the present tidal current is too weak to form sand banks (no sediment transport occurs under the present tidal current) (Collins et al., 1995). The evolution of sand banks and sand waves can be modeled using idealized morphological models. The model investigates if wavy bed patterns are developing as free instabilities of the system. The model studies the behaviour of a small bottom perturbation evolving on a basic state consisting of a tidal flow (2DH) over a flat sandy seabed. Friction and Coriolis forces, cause a net sediment transport towards the crest of the bed pattern, resulting in growth of the bed feature. Huthnance (1982a,b) was the first to treat the tidal current and the erodible sand bed as a coupled system, and predicts a preferred initial growth of bed form perturbations with their crests turned slightly anti-clockwise with respect to the current direction. De Vriend (1990) extended this research by including suspended sediment transport and the influence of wave effects. Hulscher et al.(1993) adapted the model by allowing for elliptical tidal currents (Huthnance used a unidirectional tide).

We focused on the two activities sand mining and offshore wind farms because in the coming years, large-scale sand mining is planned in the North Sea(e.g. due to the expansion of the Rotterdam harbour, extracting 365 Mm³ sand from the seabed) and numerous plans exist to build large wind farms in the North Sea.

To investigate the effects of these two activities on the North Sea seabed, we set up a GIS (Geographical Information System) containing data on the North Sea and embedded an idealized morphodynamic model to calculate the large-scale morphodynamics due to sand mining and offshore wind farms in the GIS.

2 GEOGRAPHICAL INFORMATION SYSTEM (GIS)

The main motivation to use a GIS (Geographical Information System) is that the data can be kept in a data base structure, which allows easy access and modification. Also, the dataset has a geographical nature, and the GIS is especially designed to handle geo-referenced data and can easily transform data that has a different spatial reference system. The GIS can manage the preprocessing of the data before it enters the model (e.g. perform averaging operations etc.).

The morphodynamic models to predict the effects of sand pits and wind farms on the seabed are coded in a Matlab environment. To be able to work with it in ARCGIS, a Dynamic Link Library (DLL) technique is used to convert the Matlab code to a COM object. This is an object that can be used by many coding languages. This object is imported in the Visual Basic script that is imbedded in the GIS to allow for the inclusion of a sand pit or wind farm. This code enables the user to draw a pit or farm with specified dimensions at any chosen location in the North Sea. The model then calculates the morphological effects of the presence of the sand pit or wind farm at this specific location.

3 DATA

Different data layers have to be imported into the GIS, to be able to give the morphodynamic model the site-specific input parameters they require. The quality of the results of the models depends on the accuracy of the data included in the GIS. When more accurate data becomes available, this can readily be imported in the GIS, thereby improving the accuracy of the model results.

The data on the velocity of the M2 tidal component (U (max. flow velocity M2 component), ϕ (angle of max. flow with respect to the North)) is interpolated from a grid of points provided by the RIKZ (Rijksinstituut voor Kust en Zee) and is derived from model runs of the ZUNOWAQ model (Van Dijk and Plieger, 1988). The water depth (H) data was taken from Hulscher and Van den Brink (2001) and originated from Boon and Gerritsen (1997) and Ten Brummelhuis (1997). The median grain size (d_{50}) distribution of the Southern North Sea was taken from different geographical maps (Rijks Geologische Dienst, 1984; Hydrographer of the Navy, 1992). Additional data on d_{50} for the Dutch part of the North Sea was provided by TNO-NITG.

4 SAND PITS

Under current legislation, sand extraction is only allowed outside the established -20 m NAP contour and the maximum pit depth is 2 m. For pits larger than 10 Mm³ or if the extraction area is larger than 5 Mm², an Environment Impact Assessment (EIA) is required. In this case a pit depth larger than 2 m is possible if the EIA shows that this is acceptable (Hommes et al., 2007). Changes that are likely to occur in large-scale sand extraction in the future are that several pits will be grouped together in one area, the pit volume exceeds 100 Mm³ and the pit depth may be larger than 2 m, so the surface area of the pit can stay smaller (Hoogewoning and Boers, 2001).

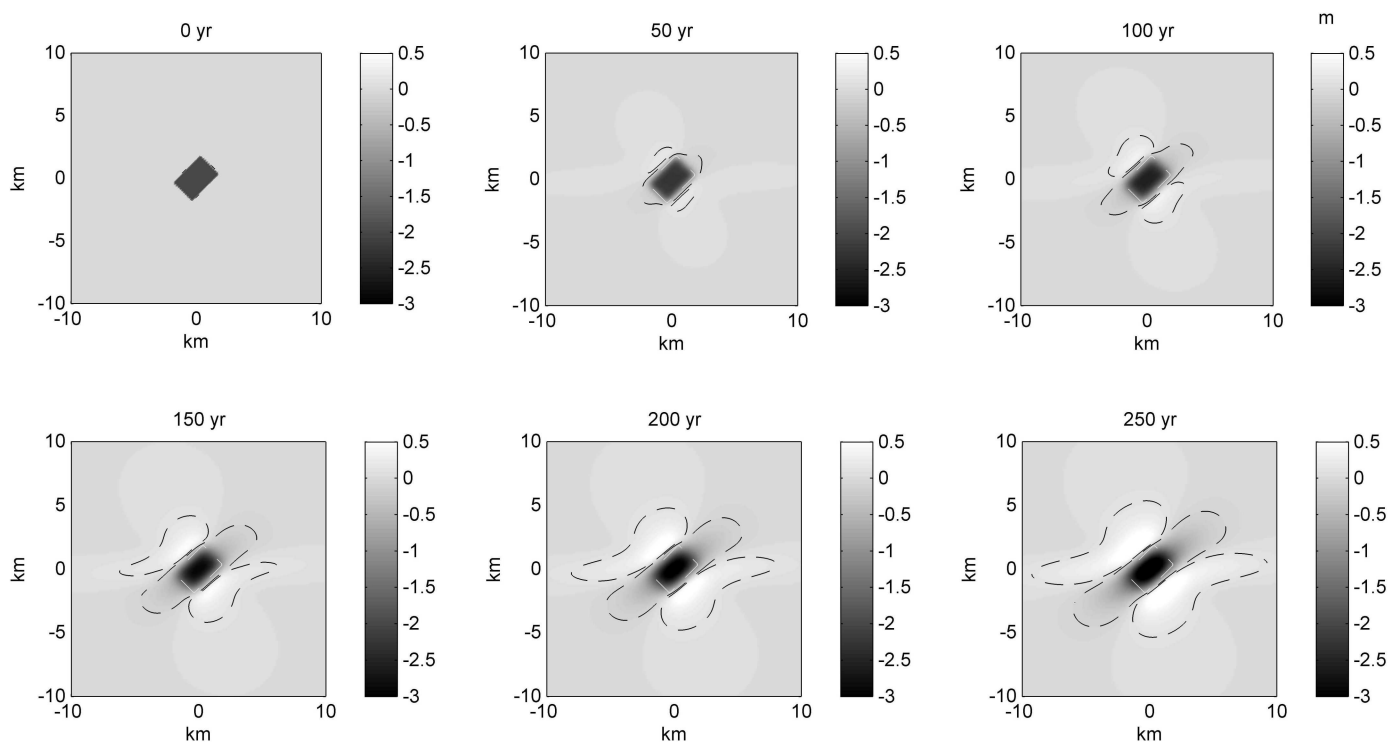


Figure 2: Time series of a sand pit of 2 x 3 km, depth 2m, water depth 25m, flow velocity 0.7 m/s and an angle with respect to the flow of 45 degrees. The time is denoted at the top of the plots (in years). The dotted line denotes the area of influence. In these plots, the flow direction is along the x-axis.

Figure 2 shows the typical development of a sandpit in time. At the initial situation, the surrounding seabed is flat. As time goes by, a pattern of banks and troughs emerges around the pit, and the pit itself deepens and deforms. The flow mechanism is as follows; when the flow reaches the pit, the cross pit flow decreases due to continuity, the along pit flow increases due to a decrease in friction, causing a deflection in the flow. The flow is influenced by the Coriolis force, which tends to enhance clockwise rotations in the North Sea. This leads to the forming of circulation zones in the area of the pit, causing a pattern of banks and troughs to appear (Roos and Hulscher, 2003).

4.1 Case study: sand extraction to facilitate the enlargement of the Rotterdam harbour

Maasvlakte 2 is the extension of the Rotterdam harbour into the North Sea. The new area will be 20 Mm² large and positioned next to relatively deep water (>20m), to facilitate easy access from sea. To claim the land from the sea a combination of soft (beach and dunes) and hard (dikes) sea defenses will be constructed and also sand is needed to raise the land above sea level. The sand that is needed for the beach and dunes and the heightening of the site will mainly come from the North Sea seabed, in total requiring 365 Mm³ of sediment. The sand will be extracted from an area in front of the location of the

harbour extension, the water depth in this area varies from 20 to 25 m. Since the volume of extracted sand is very large, the developers aim to create pits with a larger depth than is allowed under current legislation, namely, pits with a depth up to 20 m with respect to the surrounding seabed. The developers state that since there is very little equipment that can extract sand from this depth, the extraction depth in practice will be between a maximum of 10 to 15 m below the seabed (Havenbedrijf Rotterdam, 2007).

To investigate the effects of this large-scale sand extraction in the North Sea, several scenarios are calculated. The first three scenarios (a,b and c) denote an elongated pit with different orientations with respect to the flow, the pit depth is limited to the current restrictions of 2m. The fourth scenario (d) is one square pit limited to the current restrictions of 2 m depth, this means that the pit is almost 14 by 14 km wide. The fifth scenario (e) denotes a square pit with a deeper extraction namely, a depth of 4m. Roos et al.(2004) showed that the linear approximation works well for amplitudes (pit depth + changes in the seabed) up to 20% of the water depth. This means that the maximum pit depth that we can calculate in this area is about 4 m. For pits that are deeper, non-linear processes can play a role and the results of the linear model may be inaccurate. The sixth scenario (f) represents the situation where four pits are located near each other (the centers of the pits are 15 km apart).

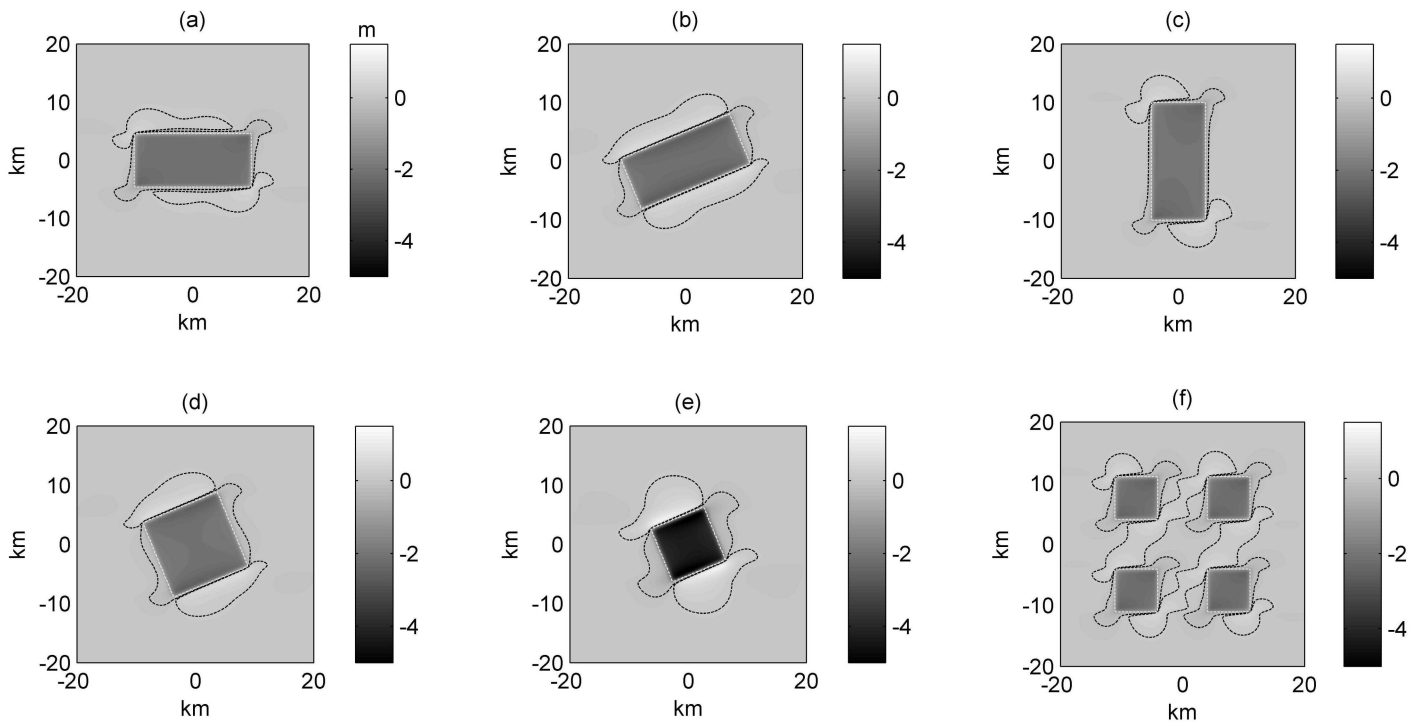


Figure 3: Overview of bed development after 100 years for different design options for a sand extraction volume of 365 Mm³, the numbers correspond to the pit numbers of

Table 1: Overview of results for different design options for a sand extraction volume of 365 Mm³.

Pit	Length M	Width m	Depth m	Orientation °	#	Area of infl km ²
a	20000	9125	2	0	1	224.3
b	20000	9125	2	22.5	1	284.8
c	20000	9125	2	90	1	215.5
d	13509	13509	2	22.5	1	240.3
e	9552	9552	4	22.5	1	368.6
f	6755	6755	2	0	4	451.0

Table 1 shows an overview of the scenario's. Figure 3 shows the results of the different scenarios after 100 years. As can be seen, a deeper pit (e) has a significantly larger effect on the surrounding seabed than a shallow pit (d). And if more than one pit is present (f), the area of influence is larger than if a single pit is used. The scenario that causes the smallest effect on the surrounding seabed is the elongated pit placed with the long side (L) perpendicular to the flow (c).

Figure 4 denotes the area of influence of a standard pit if site-specific parameters are used. The figure shows that a sand pit in front of the East Anglian coast (UK) has the largest morphological impact. At some places in this area, the area of influence is very high (>200 km²), this is due to the high flow velocities in this area, which have a large impact on the area of influence, as was also shown in the sensitivity analysis. In a large part of the North Sea, the

value of the area of influence lies between 0 and 40 km², this means that the morphological impact of a pit in this area is rather limited.

4.2 North Sea coverage; sand pits

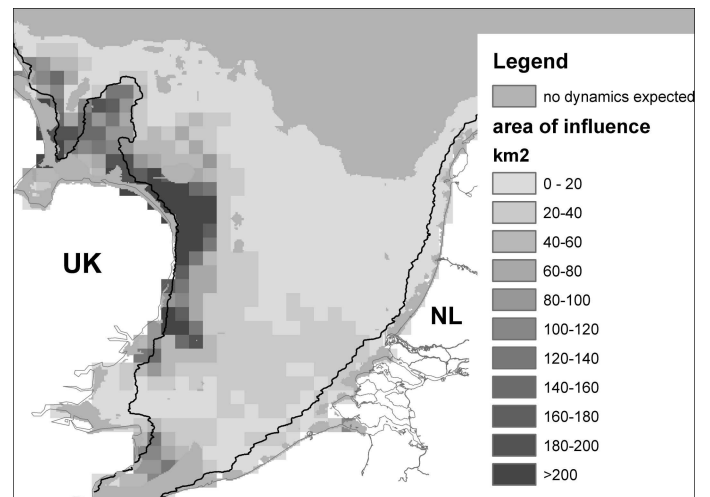


Figure 4: Overview of the area of influence of a standard pit (3 x 2 km wide, depth 2 m, angle with respect to the flow 45°) with site-specific input parameters (water depth and flow velocity). The black line denotes the 20 meter depth contour.

In Figure 4, the black line denotes the 20 m depth contour. Since we use a linear model, the depth of the pit has to be small compared to the water depth. Under the current legislation with a maximum pit depth of 2 meter this condition is generally met outside the 20 m depth contour. Also, it is currently not

allowed to extract sediment from within this contour.

5 WIND FARMS

There are many plans to build offshore wind farms in the North Sea environment. Advantages of offshore wind energy are the strong and predictable wind speeds, the energy generating capacity offshore being approximately 40% higher than onshore. Disadvantages are the higher costs for realizing and maintaining an offshore wind farm, difficulties of transporting the energy onshore and the unknown effects of wind farms on their environment (EWEA, undated). An offshore wind farm can influence the environment in several ways. There is the possible effect on birds as the presence of a wind farm can cause casualties because birds collide with the turbines. Also, the presence of a wind farm may alter the course of the flight path of migration and feeding routes of birds. The noise and vibrations of a wind farm can affect the communication of sea mammals. By legislation, wind farm areas are closed for fishing activities, thus possibly creating a safe haven effect, also the substrate that is placed as an anticour layer around the piles may form a sort of artificial reef, attracting other species of macrobenthos and fish. Offshore wind farms that are located near the shore may be visible from the coast, thereby changing the open character of the environment (Stichting de Noordzee, 2002). Finally, the offshore wind farm may have influence on the large scale morphology.

As it has only recently become technically possible to build wind farms in the offshore area, little research has been done at the effects of offshore wind farms on their environment.

5.1 Representation of a wind farm in the morphodynamic model

The wind farm can be seen as a set of piles protruding from the seabed and reaching high above the water level. In literature, two different types of research calculate the effects of the resistance of piles on the flow. In the first type, rods are used to adjust to friction in scale experiments, as the roughness is not scaled proportionally in models that are not full scale (Van den Berg and de Vries, 1979). The second type of modeling originates from the research into the effects of vegetation on the flow (Copeland, 2000; Van Velzen et al., 2002; Huthoff and Augustijn, 2006). In this chapter we will use the approach of Van Velzen et al. (2002) and adapt it for the piles of offshore wind turbines.

It is complicated to fully represent all details of the wind farm in the morphological model. Therefore, we aim at inclusion of the large-scale effects of wind farms through a local change in flow resistance

at the location of the wind farm, which is included in the shallow water equations (see Figure 5).

The flow resistance term due to a wind farm is determined by considering the spatial average of the drag force of a single wind turbine, which is given by:

$$\bar{F}_{wt} = \frac{1}{2} \rho A C_{D_wt} |\bar{U}| \bar{U} \quad (\text{Van Velzen et al., 2002}), \quad (1)$$

where A ($d_{wt}H$) is the area of the wind turbine normal to the flow direction, C_{D_wt} the drag coefficient of a cylinder, ρ the density of seawater (1025 kg/m^3) and U the site-specific flow velocity.

The drag coefficient (C_{D_wt}) depends on the Reynolds Number, defined by:

$$\text{Re} = \frac{U d_{wt}}{\nu}, \quad (2)$$

in which ν is the kinematic viscosity of seawater ($1.17 \cdot 10^{-6} \text{ m}^2/\text{s}$), d_{wt} the diameter of a wind turbine and U the site-specific flow velocity.

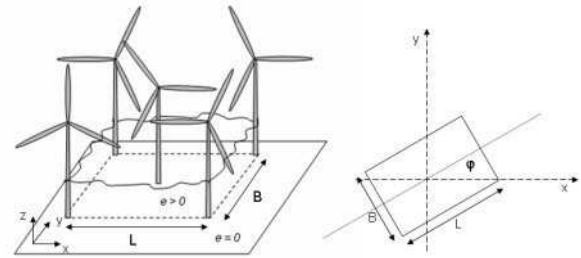


Figure 5: Representation of the wind farm in the morphological model.

To calculate the drag force per area of a complete wind farm, the drag force of a single turbine is multiplied by the number of wind turbines per square meter (N):

$$N = \frac{1}{G^2}, \quad (3)$$

where G is the average spacing between the turbines. To incorporate this frictional term in the 2DH shallow water equations, we depth-average the term \bar{F}_{wt} (equation (1)) and divide it by ρ , leading to:

$$\frac{\bar{F}_{wt}}{\rho G^2} = e |\bar{u}| \bar{u} \quad \text{in which} \quad e = \frac{d_{wt} C_{D_wt}}{2G^2} \quad (4)$$

Expressed in terms of depth-averaged flow velocity (u).

Bottom friction is represented by a widely used linearized expression (Zimmerman, 1982). As the flow resistance term is a new addition to the set of equations, and in the original use (Van Velzen et al., 2002) is used in a non-linear way, we do not linearize this term to keep close to the original notation.

As the value of the flow resistance due to the wind farm (e) is small, it is not expected that this has a big influence.

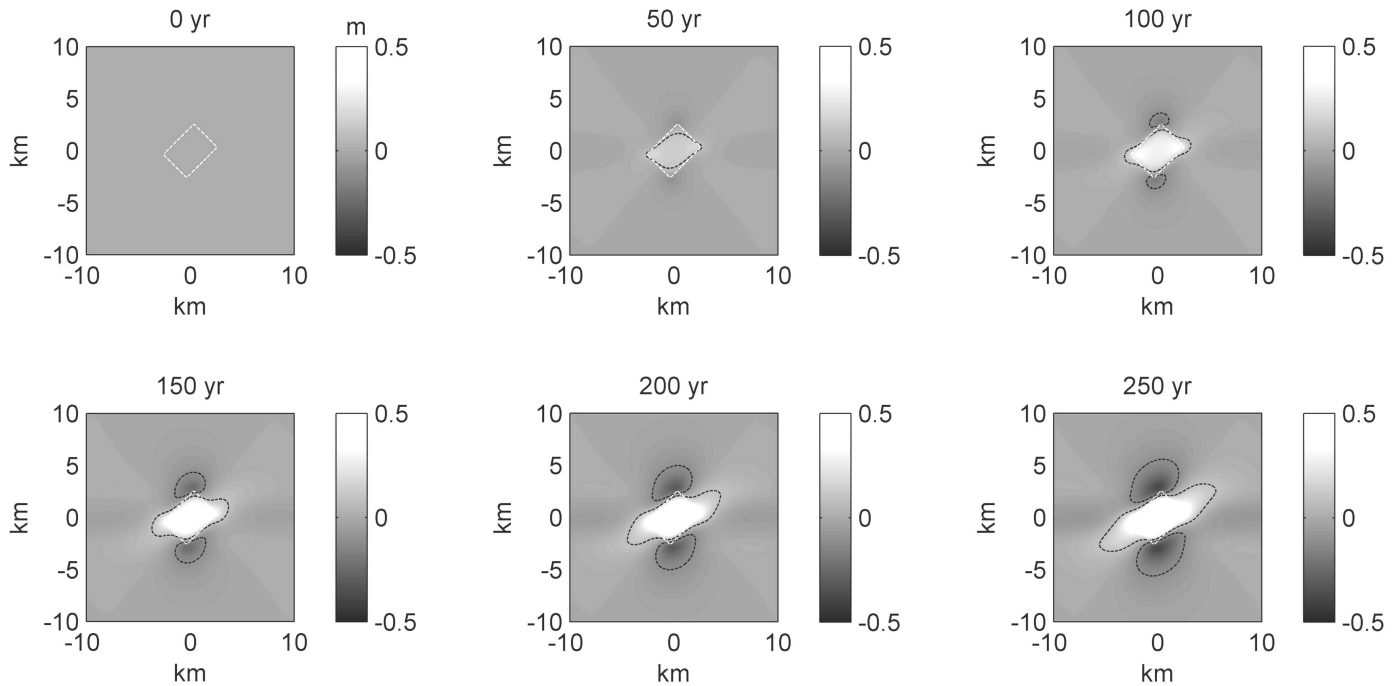


Figure 6: Timeseries of a wind farm of 3 by 4 km, spacing turbines: 500m, diameter turbines: 4.5 m, flow velocity: 0.7 m/s, water depth: 30 m, median grain size: 200 μm and an angle with respect to the flow of 45°. The white line denotes the shape of the wind farm and the black dashed line shows the area of influence. The time that has elapsed is noted at the top of the plots.

5.2 Seabed evolution due to wind farms

Figure 6 shows the development of the seabed due to a wind farm in time. At 0 years, just after the construction, the surrounding seabed is flat. As time goes by, a pattern of banks and troughs emerges around the farm. This pattern is caused by the fact that the flow is diverted due to the increased flow friction at the wind farm. As a result of this flow diversion, the seabed starts to rise at the center of the wind farm. The deflected flow is influenced by the Coriolis force, thereby causing a net imbalance over a tidal cycle and thus a net flow, causing the emerging bed features to grow. (Zimmerman, 1981; Roos and Hulscher, 2003) Several of these circulation cells may form and the number of cells that evolve is dependent on the characteristics of the wind farm.

5.3 Two cases; Humber Gateway and Q7 wind farm

By implementing the model in a GIS environment, the model allows us to calculate the effects of a wind farm using site-specific input parameters.

We selected two cases to calculate the effect of a wind farm on the seabed. These cases are listed in Table 2.

In Figure 7, the morphological effects of the Humber wind farm and the Q7 wind farm after 100 year are shown. We observe that the effects of the wind farm located off the coast of IJmuiden (Q7) ($A_{i \text{ farm}}: 13.5 \text{ km}^2$) are much smaller than the effects of the Humber wind farm ($A_{i \text{ farm}}: 191,1 \text{ km}^2$). The

morphological development is much faster for the Humber wind farm than for the Q7 wind farm.

Table 2: Overview of local parameters of the wind farms Humber Gateway and Q7.

Name	Humber Gateway	Q7
location	Mouth of the Humber (UK)	IJmuiden (NL)
#turbines	70(G=700 m)	60(G=500 m)
L (km)	7.5	4.5
B (km)	4.5	3
u (m/s)	0.86	0.58
d50 (μm)	750	375
H (m)	25	21
Theta ($^\circ$)	25	150
d_{wt} (m)	4.5	4.5
$C_{D \text{ wt}}$	0.64	0.53

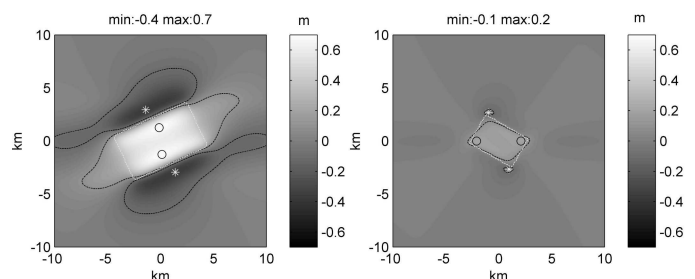


Figure 7: Seabed change in meter due to the Humber wind farm (left) and the Q7 wind farm (right) after 100 year. The values above the plot denote the lowest point of the seabed (min) and the highest bed elevation (max). The gray line denotes the wind farm and the black dashed line shows the area of influence.

5.4 North Sea overview; wind farms

Figure 8 shows the area of influence of a wind farm when site-specific parameters are used. As can be seen, in front of the East Anglian coast (UK) the area of influence of a wind farm is much larger than in the rest of the Southern North Sea, which shows that the morphological impact due to a wind farm is much larger in this area.

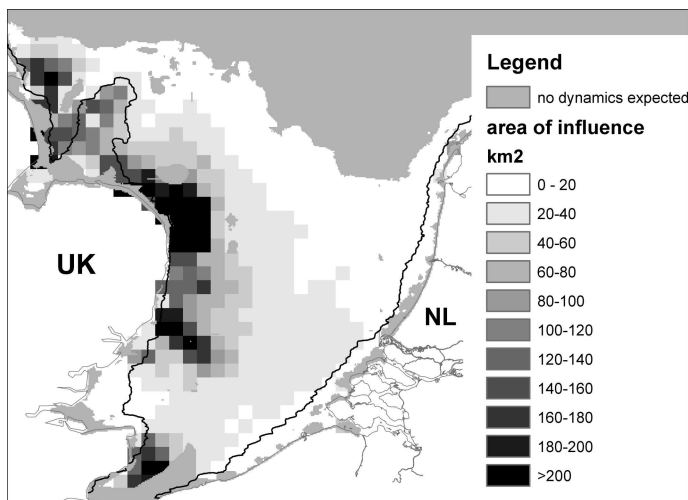


Figure 8: Overview of the area of influence of a wind farm (4.5 x 3 km, spacing 500 m diameter of the turbines 4.5 m, an angle with respect to the flow of 45 °) after 100 year. With locally defined input parameters (water depth, flow velocity and grain size). The black line denotes the -20 m NAP contour.

6 DISCUSSION

Since we implemented an idealized morphodynamic model in the GIS environment, only a limited number of hydrodynamic and sediment transport processes are included in the model (e.g. wave influence is not included).

In the models only bed load sediment transport is considered. Suspended sediment transport may alter the patterns that emerge around a disturbance due to the relaxation time of the sediment. Since we focus on offshore conditions, we assume that the bed load transport will be the dominant mode of sediment transport.

In the model the M2 tidal flow is represented by an alternating symmetrical uniform flow (block flow). Huthnance (1982a) showed that the block flow gives qualitatively similar results to an sinusoidal M2-tidal forcing. Since the flow is modeled flowing in one direction at the maximum speed of the observed M2 flow velocity one half of the tidal cycle and in the reverse direction the other half of the cycle, the flow velocity may be over estimated. And since the sediment transport is linked in a non-linear (increasing) way to the flow velocity, also the sediment transport may be overestimated. This means that in reality the morphological development may be slower than predicted. However, Latteux (1995) introduced the morphological tide. Due to the

non-linearity between the flow velocity and the sediment transport, the spring-neap cycle and other long term cycles may have a relative large influence on the morphological development. The morphological tide represents the complex tide with many components by a single representative tide which may be 6 to 20% higher than the mean tidal range. This would mean that the sediment transport due to the alternating block flow gives results that resemble the actual sediment transport rates. As we implemented a symmetrical block flow, no residual current is present, which implies that the model predicts no migration of the emerging bed patterns.

The boundaries of the model are set infinitely far away, thus applying to offshore conditions. Therefore, the model cannot predict the possible effects of human influences on the coast.

Since we used a linear morphodynamic model to predict the effects of human activities on the North Sea seabed. This means that only the initial interaction between the bed and the flow is taken into account. Therefore, we can only study the effect of human activities for small bed amplitudes (up to 20% of the water depth (Roos and Hulscher, 2007)). If the bed perturbations grow larger, non-linear processes cannot be neglected anymore. Because the model is linear, no predictions can be made about the equilibrium state of the seabed.

The models assume a flat bed in the initial situation, this means that large-scale bed forms that are initially present on the seabed (sand banks, sand waves and shore-face connected ridges) are not explicitly taken into account. The grid of the data layer of depth in the southern part of the North Sea is quite coarse so these features also do not show up in the data. It is important to note however, that the morphological behaviour of a sand pit or wind farm may change due to interaction with the surrounding bed features as is shown by De Swart and Calvete (2003) and Roos and Hulscher (2007).

If the seabed at a certain location is not sensitive to sand bank instabilities (Hulscher et al., 1993), it is not likely that the 2DH model underlying the sand pit and wind farm development will be active. In the gray areas, the model that predicts the occurrence of sand banks in the North Sea (Figure 4 and Figure 8), does not predict the occurrence of sand banks. Since the models that predict the effects of human influences are based on the model that describes the evolution of sand banks, this implies that when no sand banks are predicted, the (2DH) flow conditions that determine sand bank evolution and thus the morphodynamics due to human activities are not present in that part of the North Sea. This means that at those locations no morphological development is expected and therefore the area of influence is zero.

As measurements of large-scale offshore sand extraction and offshore wind farms are not available at

the moment, it is difficult to validate the models that predict the effects of human activities.

7 CONCLUSIONS

The results show that sand mining and wind farms have a large impact on the morphodynamics of the seabed. Furthermore, the inclusion of the morphodynamic models in the GIS allows a rapid calculation of the morphological effects of these activities at a certain location in the North Sea, thus providing a rapid assessment tool regarding the large-scale morphological effects of sand mining and offshore wind farms. Also, the GIS and the connected models form a flexible system that can be updated with new data sources and other models if these become available. These properties make the system both generic as flexible as it allows the use of the system when new data or models become available.

ACKNOWLEDGEMENTS

This research is part of the project PhD@Sea, which is substantially funded under the BSIK-programme of the Dutch Government and supported by the consortium WE@Sea. We thank Pieter Roos for his help with the modelling.

REFERENCES

- Boon, J. G. and H. Gerritsen (1997), Modelling of suspended particulate matter (SPM) in the North Sea: A dedicated orthogonal boundary-fitted modelling approach (PROMISE). Res.Rep. Z2025, Delft Hydraulics, Delft, The Netherlands.
- Collins, M. B., S. J. Shimwell, S. Gao, H. Powell, C. Hewitson and J. A. Taylor (1995). *Water and sediment movement in the vicinity of linear sandbanks: the Norfolk Banks, southern North Sea*. Marine Geology **123**: 125-142.
- Copeland, R. R. (2000), US Army Corps of Engineers. Determination of flow resistance coefficients due to shrubs and woody vegetation.
- De Swart, H. E. and D. Calvete (2003). *Non-linear response of shoreface-connected sand ridges to interventions*. Ocean Dynamics **53**: 270-277, doi 10.1007/s10236-003-0044-9.
- De Vriend, H. J. (1990). Morphological processes in shallow tidal seas. *Residual Currents and Long Term Transport*. R. T. Cheng. New York, Springer-Verlag. **38**: 276-301.
- Dyer, K. R. and D. A. Huntley (1999). *The origin, classification and modeling of sand banks and ridges*. Continental Shelf Research **19**: 1285-1330.
- Havenbedrijf_Rotterdam (2007), Environmental Impact Assessment for construction of Maasvlakte 2. Havenbedrijf Rotterdam.
- Hommel, S., S. J. M. H. Hulscher and A. Stolk (2007). *Parallel modelling approach to assess morphological impacts of offshore sand extraction*. Journal of Coastal Research **23**(6): 1565-1579. doi: 10.2112/06-0698.
- Hoogewoning, S. E. and M. Boers (2001), Fysische effecten van zeezandwinning (in Dutch). Rijksinstituut voor Kust en Zee (RIKZ), Directoraat-Generaal Rijkswaterstaat, Ministerie van Verkeer en Waterstaat.
- Hulscher, S. J. M. H., H. E. De Swart and H. J. De Vriend (1993). *The generation of offshore tidal sand banks and sand waves*. Continental Shelf Research **101**(C9): 1183-1204.
- Hulscher, S. J. M. H. and G. M. Van den Brink (2001). *Comparison between predicted and observed sand waves and sand banks in the North Sea*. Journal of Geophysical Research **106**(C5): 9327-9338.
- Huthnance, J. (1982a). *On one mechanism forming linear sandbanks*. Estuarine, Coastal and Shelf Science **14**: 79-99.
- Huthnance, J. (1982b). *On the formation of sand banks of finite extent*. Estuarine, Coastal and Shelf Science **15**: 277-299.
- Huthoff, F. and D. C. M. Augustijn (2006), Hydraulic resistance of vegetation, predictions of average flow velocities based on a rigid cylinders analogy. CE&M research report 2006R-001/WEM-003, Civil Engineering & Management Reserach Report. University of Twente.
- Hydrographer_of_the_Navy (1992). *Spurn, East Anglia: Associated British Ports; Thames estuary, Taunton, Engl., U.K.*
- Latteux, B. (1995). *Techniques for long-term morphological simulation under tidal action*. Marine Geology **126**: 129-141. SSDI 0025-3227(95)00069-0.
- Rijks_Geologische_Dienst (1984), Geological charts of the North Sea: Indefatigable, Flemish Bight, Ostend. Haarlem, The Netherlands.
- Roos, P. C. and S. J. M. H. Hulscher (2003). *Large-scale seabed dynamics in offshore morphology: modelling human intervention*. Reviews of Geophysics **41**(2): 10100, doi:10.1029/2002RG000120.
- Roos, P. C. and S. J. M. H. Hulscher (2007). *Nonlinear modeling of tidal sandbanks: wavelength evolution and sand extraction*. J. McKee Smith (ed.), Proc. of the 30th International conference on Coastal Engineering (ICCE 2006), San Diego, US, 2761-2771.
- Roos, P. C., S. J. M. H. Hulscher and H. J. De Vriend (2007). *Modelling the morphodynamic impact of offshore sandpit geometries*. Coastal Engineering **submitted**.
- Roos, P. C., S. J. M. H. Hulscher, M. A. F. Knaapen and R. M. J. Van Damme (2004). *The cross-sectional shape of tidal sand banks. Modelling and observations*. J. Geophys. Res. **109**(F2): F02003. doi:10.1029/2003JF000070.
- Stichting_de_Noordzee (2002), Frisse zeewind. Visie van de natuur- en milieuorganisaties op de ontwikkeling van windturbineparken offshore.
- Ten Brummelhuis, P. G. J., H. Gerritsen and T. Van der Kaay (1997), Sensitivity analysis and calibration of the orthogonal boundary-fitted coordinate model PROMISE for tidal flow: The use of adjoint modelling techniques. Res. Rep. Z2025, Delft Hydraulics, Delft, The Netherlands.
- Van den Berg, J. and M. de Vries (1979). *Principles of River Engineering. the non tidal alluvial river*, Pitman Publishing Limited.
- Van Dijk, R. and R. Plieger (1988), Definitieve versie ZUNOWAK model (in Dutch). GWA0-88.381, Rijkswaterstaat, Dienst Getijdewateren, The Hague, The Netherlands.
- Van Velzen, E. H., P. Jesse, P. Cornelissen and H. Coops (2002), RIZA. Stromingsweerstand vegetatie in uiterwaarden. Deel 2 achtergronddocument versie 1.0.
- Zimmerman, J. T. F. (1981). *Dynamics, diffusion and geomorphological significance of tidal residual eddies*. Nature **250**: 549-555.
- Zimmerman, J. T. F. (1982). *On the Lorentz linearization of a quadratically damped force oscillator*. Physics Letters A **89**: 123-124.